HHS Public Access

Author manuscript

J Neurointerv Surg. Author manuscript; available in PMC 2016 March 15.

Published in final edited form as:

J Neurointerv Surg. 2016 January ; 8(1): 104–110. doi:10.1136/neurintsurg-2014-011477.

Hemodynamic-Morphological Discriminant Models for Intracranial Aneurysm Rupture Remain Stable with Increasing Sample Size

Jianping Xiang, PhD[1,2,3], **Jihnhee Yu, PhD**[4], **Kenneth V. Snyder, MD, PhD**[1,3,5], **Elad I. Levy, MD**[1,3,5], **Adnan H. Siddiqui, MD, PhD**[1,3,5], and **Hui Meng, PhD**[1,2,3]

[1]Toshiba Stroke and Vascular Research Center, University at Buffalo, State University of New York; Buffalo, NY USA

[2]Department of Mechanical and Aerospace Engineering, University at Buffalo, State University of New York; Buffalo, NY USA

[3]Department of Neurosurgery, University at Buffalo, State University of New York; Buffalo, NY USA

[4]Department of Biostatistics, University at Buffalo, State University of New York; Buffalo, NY USA

[5]Department of Radiology, University at Buffalo, State University of New York; Buffalo, NY USA

Abstract

Background—We previously established three logistic regression models for discriminating intracranial aneurysm rupture status based on morphological and hemodynamic analysis of 119

Correspondence: Hui Meng PhD, Toshiba Stroke and Vascular Research Center, University at Buffalo, State University of New York, 875 Ellicott Street, Buffalo, NY 14203, Tel:716-829-3595/Fax:716-829-2212/ huimeng@buffalo.edu.

Contributorship Statement

Conception and design: Xiang, Siddiqui, Meng; Acquisition of data: all authors; Analysis and interpretation of data: Xiang, Yu, Siddiqui, Meng; Drafting the manuscript: Xiang, Meng; Critical revision of the manuscript: all authors; Final approval of the manuscript: all authors.

Data Sharing

N/A

Competing Interests Statement

Dr. Xiang: recipient of Dr. Richard J. Schlesinger grant from the American Society for Quality Biomedical Biomedical Division and principal investigator of Dawn Brejcha Chair of Research grant from Brain Aneurysm Foundation.
Dr. Yu: none.
Dr. Snyder: consultant: Toshiba; speakers' bureau: Toshiba, ev3/Covidien and The Stroke Group; honoraria: Toshiba, ev3/Covidien and The Stroke Group.
Dr. Levy: shareholder/ownership interests: Intratech Medical Ltd., Mynx/Access Closure, Blockade Medical LLC. Principal investigator: Covidien US SWIFT PRIME Trials. Other financial support: Abbott for carotid training for physicians.
Dr. Siddiqui: research grants: co-investigator of NIH grants (R01NS064592 and 5R01EB002873) and Research Development Award from the University at Buffalo; financial interests: Blockade Medical, Hotspur, Intratech Medical, Lazarus Effect, StimSox, Valor Medical; consultant: Blockade Medical, Codman & Shurtleff, Inc., Concentric Medical, ev3/Covidien Vascular Therapies, GuidePoint Global Consulting, Lazarus Effect, MicroVention, Penumbra, Stryker, Pulsar Vascular; National Steering Committee: 3D Separator Trial (Penumbra, Inc.), SWIFT PRIME Trial (Covidien), FRED Trial (MicroVention); speakers' bureau: Codman & Shurtleff, Inc.; advisory board: Codman & Shurtleff, Inc., Covidien Neurovascular; honoraria: Abbott Vascular and Codman & Shurtleff, Inc. for training other physicians in carotid stenting and endovascular stenting for aneurysms, and Penumbra, Inc.
Dr. Meng: principal investigator of NIH grant (R01NS064592), the grant from Toshiba Medical Systems and The Carol W. Harvey Memorial Chair of Research grant from Brain Aneurysm Foundation.

aneurysms (*Stroke*. 2011;42:144–152). In this study we tested if these models would remain stable with increasing sample size and investigated sample sizes required for various confidence levels.

Methods—We augmented our previous dataset of 119 aneurysms into a new dataset of 204 samples by collecting additional 85 consecutive aneurysms, on which we performed flow simulation and calculated morphological and hemodynamic parameters as done previously. We performed univariate significance tests of these parameters, and on the significant parameters we performed multivariate logistic regression. The new regression models were compared against the original models. Receiver operating characteristics analysis was applied to compare the performance of regression models. Furthermore, we performed regression analysis based on bootstrapping resampling statistical simulations to explore how many aneurysm cases were required to generate stable models.

Results—Univariate tests of the 204 aneurysms generated an identical list of significant morphological and hemodynamic parameters as previously from analysis of 119 cases. Furthermore, multivariate regression analysis produced three parsimonious predictive models that were almost identical to the previous ones; with model coefficients that had narrower confidence intervals than the original ones. Bootstrapping showed that 10%, 5%, 2%, and 1% convergence levels of confidence interval required 120, 200, 500, and 900 aneurysms, respectively.

Conclusions—Our original hemodynamic-morphological rupture prediction models are stable and improve with increasing sample size. Results from resampling statistical simulations provide guidance for designing future large multi-population studies.

Keywords

Hemodynamics; Intracranial aneurysm; Morphology; Rupture; Stability

Introduction

Intracranial aneurysms affect 5~8% of the entire population.[1] Aneurysm rupture leads to subarachnoid hemorrhage (SAH), a devastating event with high morbidity and mortality.[2] Recent advancements in neurovascular imaging have increased the detection of asymptomatic unruptured aneurysms, placing more pressure on clinicians to decide which unruptured aneurysms to treat and which to observe, since treatments are fraught with complication risks and high costs. Currently, aneurysm size is the main quantitative discriminant used in evaluating rupture risk. However, small aneurysms still account for a large portion of rupture.[3] Consequently, shape-based morphological parameters have been explored and correlated with rupture.[3–5] On the other hand, hemodynamics is found to be associated with aneurysm rupture and plays a fundamental role in mechanisms of aneurysm rupture.[6–12] Moreover, the recently released American Heart/Stroke Association guidelines for aneurysm management recommend that clinicians "consider morphological and hemodynamic characteristics of the aneurysm when discussing the risk of aneurysm rupture."[13]

In a study of 119 aneurysms,[8] we identified morphological and hemodynamic factors that discriminate ruptured from unruptured aneurysms and, through multivariate logistic regression analysis, built 3 aneurysm rupture probability models based on morphology only,

hemodynamics only and combined parameters. High probability of rupture status was found to be associated with larger size ratio (SR) in the morphological model, lower aneurysm-averaged wall shear stress (WSS) and higher aneurysm-averaged oscillatory shear index (OSI) in the hemodynamic model, and all three in the combined model. In this follow-up study we asked the following questions: (1) Would these models be different if we increase the sample size? (2) How many samples are required to build stable statistical models? The objective of the current study is to evaluate the stability of these models by answering these questions.

Methods

Study Population

We collected a new cohort of 85 aneurysms (18 ruptured; 67 unruptured) in 74 consecutive patients imaged at Millard Fillmore Gates Hospital in Buffalo, NY between 2009 and 2010 after the approval by University at Buffalo Institutional Review Board. The demographic information (age, gender, location and type) of the new cohort is shown in Table 1. This dataset was consecutive with the 119 aneurysms in our previous study.[8]

Morphological and Hemodynamic Parameter Extraction

Morphological and hemodynamic parameters for each aneurysm were calculated as previously described.[5, 8] Briefly, DICOM images were segmented at the 3D region of interest, aneurysm lumen and adjacent vessels. An in-house Matlab code was used to calculate 6 morphological parameters:[5] *Aneurysm Size*, *SR*, *Aspect Ratio* (*AR*), *Ellipticity Index* (*EI*), *Non-Sphericity Index (NSI)*, and *Undulation Index* (*UI*). For computational fluid dynamics (CFD) simulations, finite volume meshes of 0.5–1 million elements were imported into the CFD solver to calculate time-resolved 3D velocity and pressure fields. Three pulsatile cycles were simulated, with the last cycle being taken as output to ensure that numerical stability had been reached. All data presented were time-averages over the third pulsatile cycle of flow simulation when applicable. From the flow solutions, we calculated 7 hemodynamic parameters described in detail previously:[8] *WSS, Maximum WSS (MWSS), Low WSS Area Percentage (LSA), OSI, Relative Resident Time (RRT), WSS gradient (WSSG),* and *Number of Vortices (NV).* WSS is tangential frictional stress caused by blood flow on the vessel wall. In the statistical analysis, we averaged WSS over a cardiac cycle, and further averaged over the aneurysm sac. MWSS is the maximum time-averaged aneurysmal WSS magnitude. LSA is defined as areas of the aneurysm wall exposed to WSS below 10% of the mean parent arterial WSS. OSI measures the direction change of WSS during the cardiac cycle, and is defined as aneurysm-averaged OSI for quantitative analysis. RRT reflects the residence time of blood near the wall and is inversely proportional to the magnitude of the time-averaged WSS vector. WSSG measures the change of WSS magnitude in the flow direction. NV is counted based on the velocity field of the representative cross-sectional plane for each aneurysm. As with our original paper,[8] for aneurysm-averaged WSS, MWSS and RRT, we normalized them by parent vessel average values.

Stability Testing of the Predictive Models

To test the stability of our previous rupture prediction models,[8] we aggregated the new (85 aneurysms) and original (119 aneurysms) cohorts into one dataset of 204 aneurysms. Univariate significant tests (Student t test for normally distributed data or Wilcoxon rank-sum test for abnormally distributed data) of the 13 morphological and hemodynamic parameters identified significant parameters. The significant level $p<0.01$ was considered statistically significant with Bonferroni correction. Multivariate logistic regression using stepwise elimination was then applied to the significant morphological, hemodynamic, and combined parameters.[8] The new multivariate logistic regression models were compared against the original models. We tested whether the new models were comprised of the same parameters. If so, we used the confidence interval (CI) at 95% level to examine how consistent these two sets of models were. Receiver operating characteristics (ROC) analysis was applied to compare the performance of the regression models through the area under the ROC (AUC-ROC) when applicable.

Resampling Statistical Simulation

In order to know how many aneurysm cases are required to generate sufficiently stable models for the benefit of future large population aneurysm rupture risk studies, we performed a simulation study for the logistic regression analysis based on the bootstrapping resampling statistical method to investigate the convergence of CI width of the coefficients in the regression models.[14] This is conceptually similar to the grid convergence study commonly conducted in numerical simulations. Bootstrapping can assign measures of accuracy (e.g., CIs) to sample estimates.[14] It evaluates a variability of an estimator through resampling, assuming that the collected data have the same distributional properties as the original population. We carried out statistical simulations where the same set of variable entries was used in the logistic regression models (SR in the morphological model, WSS and OSI in the hemodynamic model, all three in the combined model) in the following steps:

1. From the aggregated dataset of 204 aneurysms, we carried out random sample selection for increasing sample size n (n from 30 to 1000 with increment of 20). The case selection was random and thus some cases may have been selected for multiple times.
2. At each step (n aneurysms), we randomly generated 1000 samples from the 204 aneurysms using bootstrapping replication. For each selection of n aneurysms, we performed the logistic regression and calculated CI width for the coefficients of the regression model.
3. At each step, the process was repeated 1000 times to calculate the average of CI width.
4. CI width (each step giving lower and upper limits) and relative change (difference of interval width with n aneurysms minus interval width with $n-20$ aneurysms, divided by interval width with n aneurysms) were plotted and analyzed.

All statistical analysis was done using SPSS 17.0 software (SPSS, Inc., Chicago, IL) and the R Project for Statistical Computing.

Results

Figure 1 shows aneurysm geometry, flow streamlines, WSS distribution and OSI distribution of 4 representative ruptured (top) and 4 representative unruptured (bottom) aneurysms from the new cohort. WSS distribution in Figure 1 is the pointwise time-averaged WSS distribution; while in our statistical analysis, WSS is further averaged over the aneurysm sac. Univariate testing of the 204 samples showed that aneurysm Size and the hemodynamic factor WSSG were not discriminators of rupture at the significance level of 0.01, whereas all other parameters including SR, UI, NSI, EI, AR, WSS, MWSS, OSI, LSA, RRT, and NV were significant at distinguishing ruptured from unruptured aneurysms ($p<0.001$). This finding is consistent with previous findings based on the original cohort of 119 aneurysms.[8]

Based on these significant parameters, multivariate logistic regression analysis of the aggregated cohort of 204 aneurysms generated three new risk stratification models: morphology only, hemodynamics only, and combined. The new hemodynamics-only regression model consisted of WSS and OSI as independent predictors, which is consistent with the original hemodynamic model.[8] However, the new morphology-only model included both SR and UI, whereas in the original multivariate regression model only SR was significant.[8]

To investigate the contribution of UI to the morphological model, we used SR alone to build a univariate logistic regression model from the 204 samples and compared it against the model resulting from multivariate regression containing both SR and UI. The two models had very similar AUC-ROC values (0.831 and 0.835, respectively, Figure 2). This indicates that the contribution of UI to classification of aneurysm rupture status through morphological regression models is minimal. We therefore chose the SR-alone model as the parsimonious morphological predictive model from the 204 cases.

The final parsimonious predictive models based on the aggregated 204 aneurysms for morphology only, hemodynamics only, and combined are:

$$Odd_{M}=e^{0.86\cdot SR-2.84} \quad (1)$$

$$Odd_{H}=e^{-0.58\cdot WSS+2.55\cdot OSI-0.76} \quad (2)$$

$$Odd_{Combined}=e^{0.58\cdot SR-0.33\cdot WSS+2.14\cdot OSI-2.43} \quad (3)$$

where $Odds=p/(1-p)$ is the odds and p is the probability of an aneurysm being ruptured. Comparing Equations 1–3 from 204 aneurysms against the original Equations 4–6 from the 119 aneurysms in Xiang et al,[8] we observe essentially the same 3 models with only slight differences in model coefficients. However, these coefficients have overlapping CIs for corresponding coefficients (Figure 3). Evidently, when the sample size increased from 119 to 204, the CI width at 95% level drastically decreased from 0.88 to 0.58 for SR in the morphological model; from 0.72 to 0.57 for WSS, and from 3.18 to 2.19 for OSI in the

hemodynamic model; from 1.05 to 0.67 for SR, 0.79 to 0.61 for WSS, and 3.28 to 2.20 for OSI in the combined model. Because of the decreased variability (thus increased confidence), we suggest to use the updated rupture prediction models from the 204 samples (Eq.1–3), until they are replaced by future models extracted from larger datasets or with better performance.

Results by bootstrapping resampling simulations are given in Figure 4. Figure 4A shows reduction of CI at the 95% level as the number of samples was increased, while Figure 4B demonstrated the relative change of CI for the model coefficients. The model coefficients converged to their final values as more samples were added. We found that level of 10%, 5%, 2%, and 1% CI convergences required 120, 200, 500, and 900 aneurysms, respectively. This information provided the insight for the future large sample and multi-center aneurysm rupture risk study.

Discussion

Increasing detection of unruptured aneurysms places more and more pressure on neurosurgeons and neurointerventionalists to weigh rupture risk against surgical complication risks before making treatment decisions. Aneurysmal morphology and hemodynamics show great promises for rupture risk stratifications.[3–11, 15–18] The importance of aneurysmal morphology and hemodynamics for rupture risk assessment was also stressed by American Heart and Stroke Association.[13] In our previous study of 119 aneurysms, we found that SR, WSS and OSI are independent predictors and provided three regression models for aneurysm risk stratifications, based on hemodynamics only, morphology only, and hemodynamics and morphology combined. In the current study, we demonstrated the stability of the models by comparing regression models from an augmented sample of 204 aneurysms against those from the original 119 aneurysms. The three classification models are shown to be stable and, furthermore, improve with the increasing sample size.

In the morphology category, we found that aneurysm size was not significant while AR was significant, which is consistent with findings from many other studies.[3, 5] In the final morphological model resulting from multivariate regression of the 204 samples, UI was also retained in addition to SR; however, ROC analysis indicated that the contribution of UI to the model was minimal. SR, a concept originally proposed by our group,[5, 19] has been found in many recent studies to be a significant predictor of aneurysm rupture status, regardless if SR was defined on a 3D [5, 8, 20–22] or 2D bases, [15, 23] or which linear length was adopted to measure the aneurysm "size" in the ratio calculation.[24] In a large study of 854 ruptured and 180 unruptured aneurysms, Kashiwazaki et al discovered that SR, but not the absolute aneurysm size, highly predicted rupture status in the small aneurysms (< 5 mm).[20]

In the hemodynamics category, we found that low WSS and high OSI were independently correlated with ruptured aneurysms and that a model including these two parameters provided the odds of rupture. These were exactly the same findings as from our previous analysis of 119 aneurysms.[8] Many studies have found a correlation between low WSS and ruptured aneurysms.[4, 6, 7, 25, 26] Low WSS regions are typically located at aneurysm dome,[11]

where 84% of rupture occur.[27] Low WSS and high OSI are related to "disturbed" flow,[28] which causes endothelial cells to decrease endothelial nitric oxide synthase activity, upregulates surface adhesion molecules and increases endothelial permeability. All of these promote atherogenesis and inflammatory cell infiltration.[28] Inflammation has been thought as a key mechanism for IA rupture.[29–31] Our results provide further statistical evidence supporting the association of low WSS and high OSI with rupture identified previously.[6–8]

Nevertheless, a potential role of high WSS in aneurysm rupture should not be excluded,[7] especially in small, conservatively followed aneurysms[32] and aneurysms with jet impingement in the sac.[33, 34] High WSS resulting from flow impingement on the wall has been shown to trigger aneurysm degradation as described in aneurysm initiation[35] and progression[36]. In the aneurysm cohort of the current study, a few of the ruptured aneurysms appeared to be dominated by impinging flow, but high WSS or high maximum WSS did not contribute significantly to the predictive models.

In light of the controversy and confusions surrounding whether low WSS or high WSS better predicts rupture, we have recently proposed a unified hypothesis that both low WSS and high WSS could be responsible for aneurysm growth and rupture via two independent hemodynamically driven biological pathways.[6, 7] However, it appears that more ruptured aneurysms are driven by the low WSS mechanism than the high WSS mechanism, based on many more reports of low WSS correlation with rupture [8, 10, 11, 17, 18, 25, 26, 37–40] than high WSS.[9, 33, 41, 42]

This study has also investigated how many samples are required for building stable statistical models at different convergence levels of CI. We performed regression analyses using bootstrapping resampling of 30 to 1000 aneurysms from the aggregated pool of 204 aneurysms. We have demonstrated that an increasing level of CI convergence requires an increasing numbers of aneurysm samples. The resampling statistical simulation sheds light on future multicenter and multi-population studies. It provides the guidance on the numbers of aneurysms needed to achieve certain level of convergence for CI width. For example, in order to achieve 1% convergence level for the CI width of the models, the target sample size should be around 1000 aneurysms.

This study has several limitations. First, our dataset may have a population bias, and hence our conclusions may not be valid for different patient populations. In the future, multicenter studies with larger multi-population datasets are needed to validate these models and may derive new models.[43] Secondly, our current models are limited to image-derived morphological and hemodynamic parameters. In the future, comprehensive aneurysm rupture risk statistical models should also consider other risk factors including demographic, genetic, wall-biomechanical and medical factors. Thirdly, the rupture probability calculated from our predictive models does not involve time because, like most other aneurysm rupture risk studies, ours were based on cross-sectional data and not prospective longitudinal data. Finally, aneurysm geometries may have been affected by the rupture event, although increasing evidence indicates that aneurysms do not shrink when they rupture.[5, 44]

Conclusions

The hemodynamic and morphological models for aneurysm rupture status prediction are stable and statistically significant. Augmenting the dataset improves the model coefficient estimation. Regression analysis from bootstrapping resampling statistical simulation sheds light on the design of future large and multi-center aneurysm rupture risk studies.

Acknowledgments

The authors thank Vincent M. Tutino, MS, for help on the illustrations.

Funding Statement

NIH grant-R01NS064592, a grant from Toshiba Medical Systems, and Dr. Richard J. Schlesinger grant from the American Society for Quality Biomedical Division.

Abbreviations

ACOM	anterior communicating artery
AR	aspect ratio
AUC-ROC	area under the receiver-operating-characteristic curve
BA	basilar artery
CFD	computational fluid dynamics
CI	confidence interval
EI	ellipticity index
ICA	internal carotid artery
LSA	low wall shear stress area percentage
MCA	middle cerebral artery
MWSS	maximum wall shear stress
NSI	nonsphericity index
NV	number of vortices
OSI	oscillatory shear index
PCOM	posterior communicating artery
PICA	posterior inferior cerebellar artery
RRT	relative residence time
SAH	subarachnoid hemorrhage
SR	size ratio
UI	undulation index
WSS	wall shear stress

WSSG	wall shear stress gradient
VA	vertebral artery

References

1. Rinkel GJ, Djibuti M, Algra A, van Gijn J. Prevalence and risk of rupture of intracranial aneurysms: A systematic review. Stroke; a journal of cerebral circulation. 1998; 29:251–256.
2. Cross DT 3rd, Tirschwell DL, Clark MA, Tuden D, Derdeyn CP, Moran CJ, et al. Mortality rates after subarachnoid hemorrhage: Variations according to hospital case volume in 18 states. J Neurosurg. 2003; 99:810–817. [PubMed: 14609158]
3. Ujiie H, Tachibana H, Hiramatsu O, Hazel AL, Matsumoto T, Ogasawara Y, et al. Effects of size and shape (aspect ratio) on the hemodynamics of saccular aneurysms: A possible index for surgical treatment of intracranial aneurysms. Neurosurgery. 1999; 45:119–130. [PubMed: 10414574]
4. Raghavan ML, Ma B, Harbaugh RE. Quantified aneurysm shape and rupture risk. J Neurosurg. 2005; 102:355–362. [PubMed: 15739566]
5. Dhar S, Tremmel M, Mocco J, Kim M, Yamamoto J, Siddiqui AH, et al. Morphology parameters for intracranial aneurysm rupture risk assessment. Neurosurgery. 2008; 63:185–196. discussion 196-187. [PubMed: 18797347]
6. Xiang J, Tutino VM, Snyder KV, Meng H. Cfd: Computational fluid dynamics or confounding factor dissemination? The role of hemodynamics in intracranial aneurysm rupture risk assessment. AJNR Am J Neuroradiol. 2013 Sep 12. Epub ahead of print.
7. Meng H, Tutino VM, Xiang J, Siddiqui A. High wss or low wss? Complex interactions of hemodynamics with intracranial aneurysm initiation, growth, and rupture: Toward a unifying hypothesis. AJNR Am J Neuroradiol. 2013 Jul 4. Epub ahead of print.
8. Xiang J, Natarajan SK, Tremmel M, Ma D, Mocco J, Hopkins LN, et al. Hemodynamic-morphologic discriminants for intracranial aneurysm rupture. Stroke; a journal of cerebral circulation. 2011; 42:144–152.
9. Cebral JR, Mut F, Weir J, Putman C. Quantitative characterization of the hemodynamic environment in ruptured and unruptured brain aneurysms. AJNR American journal of neuroradiology. 2011; 32:145–151. [PubMed: 21127144]
10. Jou LD, Lee DH, Morsi H, Mawad ME. Wall shear stress on ruptured and unruptured intracranial aneurysms at the internal carotid artery. AJNR Am J Neuroradiol. 2008; 29:1761–1767. [PubMed: 18599576]
11. Shojima M, Oshima M, Takagi K, Torii R, Hayakawa M, Katada K, et al. Magnitude and role of wall shear stress on cerebral aneurysm: Computational fluid dynamic study of 20 middle cerebral artery aneurysms. Stroke; a journal of cerebral circulation. 2004; 35:2500–2505.
12. Xiang J, Yu J, Choi H, Dolan Fox JM, Snyder KV, Levy EI, et al. Rupture resemblance score (rrs): Toward risk stratification of unruptured intracranial aneurysms using hemodynamic-morphological discriminants. J Neurointerv Surg. 2014
13. Connolly ES Jr, Rabinstein AA, Carhuapoma JR, Derdeyn CP, Dion J, Higashida RT, et al. Guidelines for the management of aneurysmal subarachnoid hemorrhage: A guideline for healthcare professionals from the american heart association/american stroke association. Stroke. 2012; 43:1711–1737. [PubMed: 22556195]
14. Henderson AR. The bootstrap: A technique for data-driven statistics. Using computer-intensive analyses to explore experimental data. Clinica chimica acta; international journal of clinical chemistry. 2005; 359:1–26.
15. Rahman M, Smietana J, Hauck E, Hoh B, Hopkins N, Siddiqui A, et al. Size ratio correlates with intracranial aneurysm rupture status: A prospective study. Stroke; a journal of cerebral circulation. 2010; 41:916–920.
16. Xiang J, Tremmel M, Kolega J, Levy EI, Natarajan SK, Meng H. Newtonian viscosity model could overestimate wall shear stress in intracranial aneurysm domes and underestimate rupture risk. J Neurointerv Surg. 2012; 4:351–357. [PubMed: 21990529]

17. Kawaguchi T, Nishimura S, Kanamori M, Takazawa H, Omodaka S, Sato K, et al. Distinctive flow pattern of wall shear stress and oscillatory shear index: Similarity and dissimilarity in ruptured and unruptured cerebral aneurysm blebs. Journal of neurosurgery. 2012; 117:774–780. [PubMed: 22920960]
18. Miura Y, Ishida F, Umeda Y, Tanemura H, Suzuki H, Matsushima S, et al. Low wall shear stress is independently associated with the rupture status of middle cerebral artery aneurysms. Stroke. 2013; 44:519–521. [PubMed: 23223503]
19. Tremmel M, Dhar S, Levy EI, Mocco J, Meng H. Influence of intracranial aneurysm-to-parent vessel size ratio on hemodynamics and implication for rupture: Results from a virtual experimental study. Neurosurgery. 2009; 64:622–630. discussion 630-621. [PubMed: 19349824]
20. Kashiwazaki D, Kuroda S. Sapporo SAHSG. Size ratio can highly predict rupture risk in intracranial small (<5 mm) aneurysms. Stroke; a journal of cerebral circulation. 2013; 44:2169–2173.
21. Li M, Jiang Z, Yu H, Hong T. Size ratio: A morphological factor predictive of the rupture of cerebral aneurysm? The Canadian journal of neurological sciences. Le journal canadien des sciences neurologiques. 2013; 40:366–371. [PubMed: 23603173]
22. Lin N, Ho A, Gross BA, Pieper S, Frerichs KU, Day AL, et al. Differences in simple morphological variables in ruptured and unruptured middle cerebral artery aneurysms. Journal of neurosurgery. 2012; 117:913–919. [PubMed: 22957531]
23. Ma D, Tremmel M, Paluch RA, Levy EI, Meng H, Mocco J. Size ratio for clinical assessment of intracranial aneurysm rupture risk. Neurol Res. 2010; 32:482–486. [PubMed: 20092677]
24. Lauric A, Baharoglu MI, Gao BL, Malek AM. Incremental contribution of size ratio as a discriminant for rupture status in cerebral aneurysms: Comparison with size, height, and vessel diameter. Neurosurgery. 2012; 70:944–951. discussion 951-942. [PubMed: 21997542]
25. Lu G, Huang L, Zhang XL, Wang SZ, Hong Y, Hu Z, et al. Influence of hemodynamic factors on rupture of intracranial aneurysms: Patient-specific 3d mirror aneurysms model computational fluid dynamics simulation. AJNR Am J Neuroradiol. 2011; 32:1255–1261. [PubMed: 21757526]
26. Zhang Y, Mu S, Chen J, Wang S, Li H, Yu H, et al. Hemodynamic analysis of intracranial aneurysms with daughter blebs. European neurology. 2011; 66:359–367. [PubMed: 22134355]
27. Crompton MR. Mechanism of growth and rupture in cerebral berry aneurysms. Br Med J. 1966; 1:1138–1142. [PubMed: 5932074]
28. Malek AM, Alper SL, Izumo S. Hemodynamic shear stress and its role in atherosclerosis. JAMA. 1999; 282:2035–2042. [PubMed: 10591386]
29. Chalouhi N, Hoh BL, Hasan D. Review of cerebral aneurysm formation, growth, and rupture. Stroke; a journal of cerebral circulation. 2013; 44:3613–3622.
30. Tulamo R, Frosen J, Hernesniemi J, Niemela M. Inflammatory changes in the aneurysm wall: A review. Journal of neurointerventional surgery. 2010; 2:120–130. [PubMed: 21990591]
31. Kataoka K, Taneda M, Asai T, Kinoshita A, Ito M, Kuroda R. Structural fragility and inflammatory response of ruptured cerebral aneurysms. A comparative study between ruptured and unruptured cerebral aneurysms. Stroke; a journal of cerebral circulation. 1999; 30:1396–1401.
32. Qian Y, Takao H, Umezu M, Murayama Y. Risk analysis of unruptured aneurysms using computational fluid dynamics technology: Preliminary results. AJNR Am J Neuroradiol. 2011; 32:1948–1955. [PubMed: 21903914]
33. Castro M, Putman C, Radaelli A, Frangi A, Cebral J. Hemodynamics and rupture of terminal cerebral aneurysms. Acad Radiol. 2009; 16:1201–1207. [PubMed: 19553143]
34. Cebral JR, Mut F, Weir J, Putman CM. Association of hemodynamic characteristics and cerebral aneurysm rupture. AJNR Am J Neuroradiol. 2011; 32:264–270. [PubMed: 21051508]
35. Metaxa E, Tremmel M, Natarajan SK, Xiang J, Paluch RA, Mandelbaum M, et al. Characterization of critical hemodynamics contributing to aneurysmal remodeling at the basilar terminus in a rabbit model. Stroke. 2010; 41:1774–1782. [PubMed: 20595660]
36. Hoi Y, Meng H, Woodward SH, Bendok BR, Hanel RA, Guterman LR, et al. Effects of arterial geometry on aneurysm growth: Three-dimensional computational fluid dynamics study. J Neurosurg. 2004; 101:676–681. [PubMed: 15481725]

37. Omodaka S, Sugiyama S, Inoue T, Funamoto K, Fujimura M, Shimizu H, et al. Local hemodynamics at the rupture point of cerebral aneurysms determined by computational fluid dynamics analysis. Cerebrovasc Dis. 2012; 34:121–129. [PubMed: 22965244]

38. Xu J, Yu Y, Wu X, Wu Y, Jiang C, Wang S, et al. Morphological and hemodynamic analysis of mirror posterior communicating artery aneurysms. PLoS One. 2013; 8:e55413. [PubMed: 23383184]

39. Goubergrits L, Schaller J, Kertzscher U, van den Bruck N, Poethkow K, Petz C, et al. Statistical wall shear stress maps of ruptured and unruptured middle cerebral artery aneurysms. J R Soc Interface. 2012; 9:677–688. [PubMed: 21957117]

40. Valencia A, Morales H, Rivera R, Bravo E, Galvez M. Blood flow dynamics in patient-specific cerebral aneurysm models: The relationship between wall shear stress and aneurysm area index. Med Eng Phys. 2008; 30:329–340. [PubMed: 17556005]

41. Chien A, Tateshima S, Sayre J, Castro M, Cebral J, Vinuela F. Patient-specific hemodynamic analysis of small internal carotid artery-ophthalmic artery aneurysms. Surg Neurol. 2009; 72:444–450. discussion 450. [PubMed: 19329152]

42. Chien A, Tateshima S, Castro M, Sayre J, Cebral J, Vinuela F. Patient-specific flow analysis of brain aneurysms at a single location: Comparison of hemodynamic characteristics in small aneurysms. Med Biol Eng Comput. 2008; 46:1113–1120. [PubMed: 18931868]

43. Cebral JR, Meng H. Counterpoint: Realizing the clinical utility of computational fluid dynamics--closing the gap. AJNR Am J Neuroradiol. 2012; 33:396–398. [PubMed: 22282452]

44. Rahman M, Ogilvy CS, Zipfel GJ, Derdeyn CP, Siddiqui AH, Bulsara KR, et al. Unruptured cerebral aneurysms do not shrink when they rupture: Multicenter collaborative aneurysm study group. Neurosurgery. 2011; 68:155–160. discussion 160-151. [PubMed: 21150760]

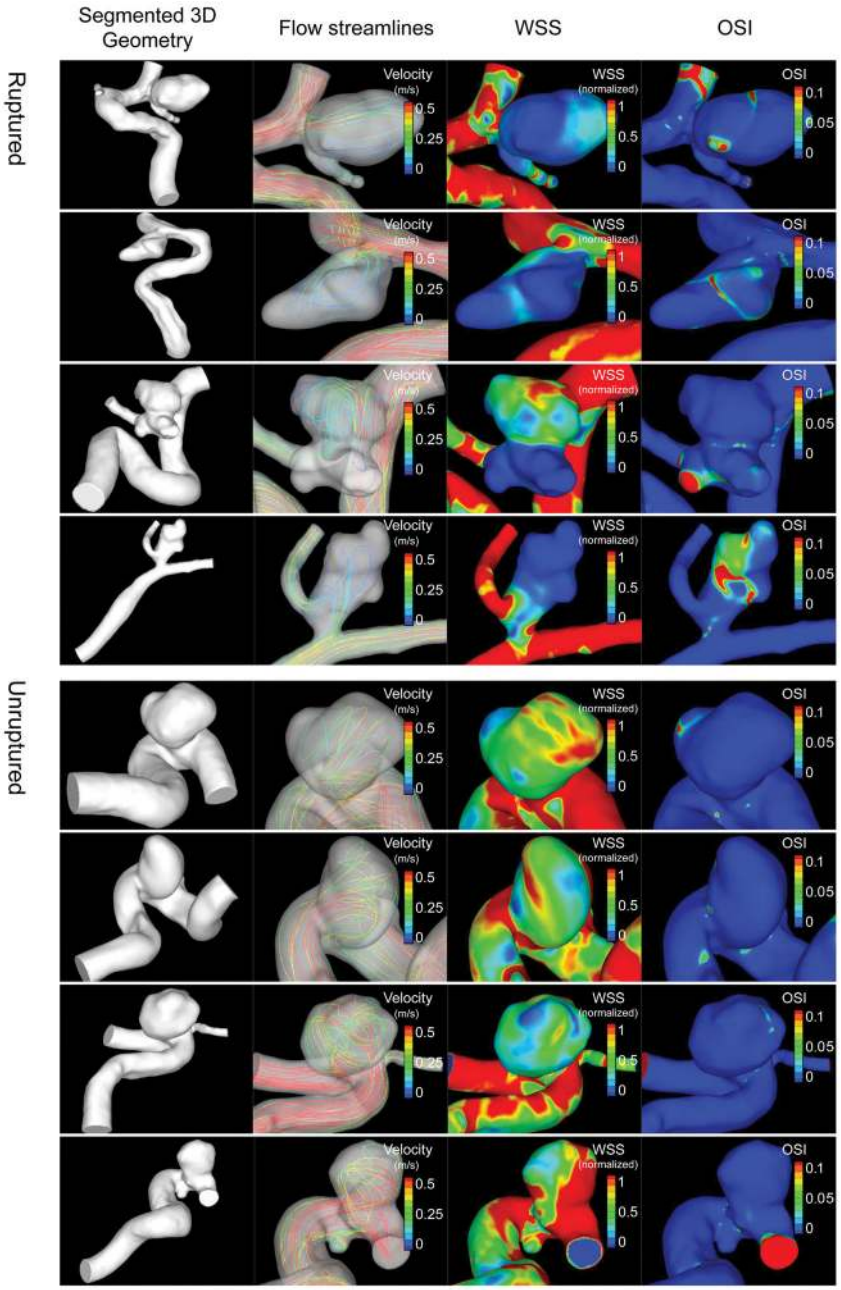

Figure 1.

Aneurysm geometry, flow streamlines, WSS distribution and OSI distribution of 4 representative ruptured (top) and 4 representative unruptured (bottom) aneurysms from the new cohort. Ruptured aneurysms showed significant higher SR, UI, AR, OSI and lower WSS than unruptured aneurysms.

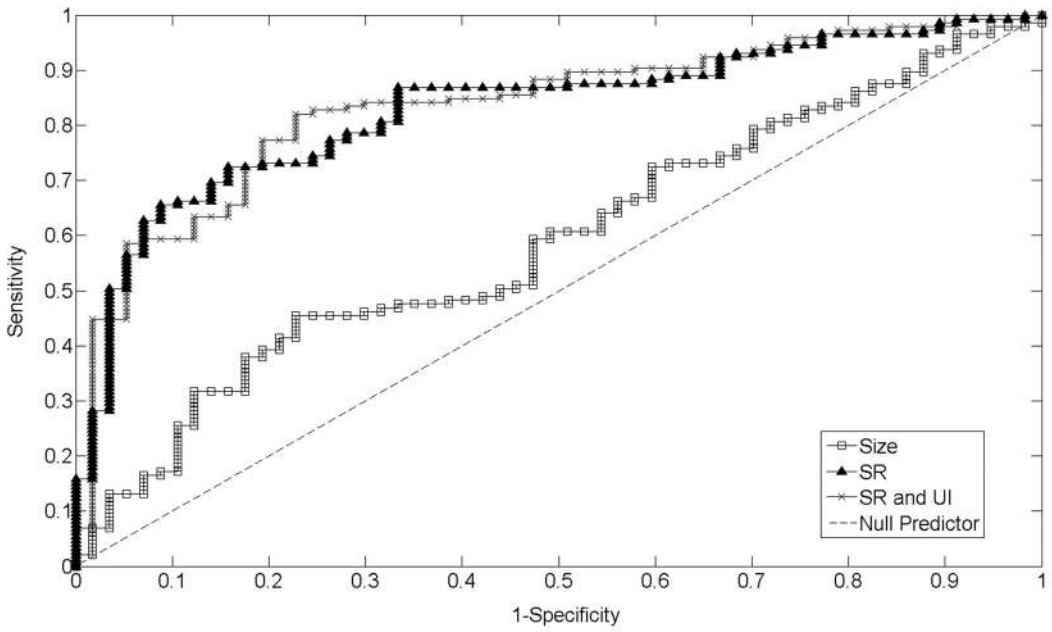

Figure 2.

ROC curves of probabilities from multiple logistic regression models based on SR alone, SR and UI, using size and null predictor as references.

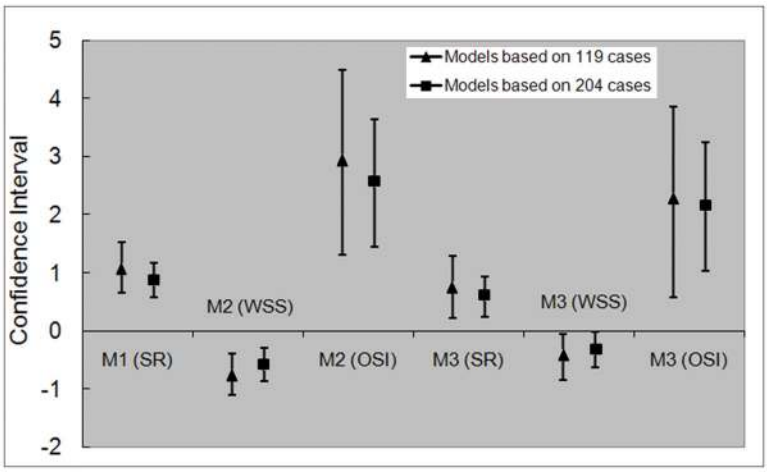

Figure 3.

CIs for the coefficients of the three regression models in the previous 119 aneurysms and aggregated 204 aneurysms. M1 = Morphological Model; M2 = Hemodynamic Model; M3 = Combined Model.

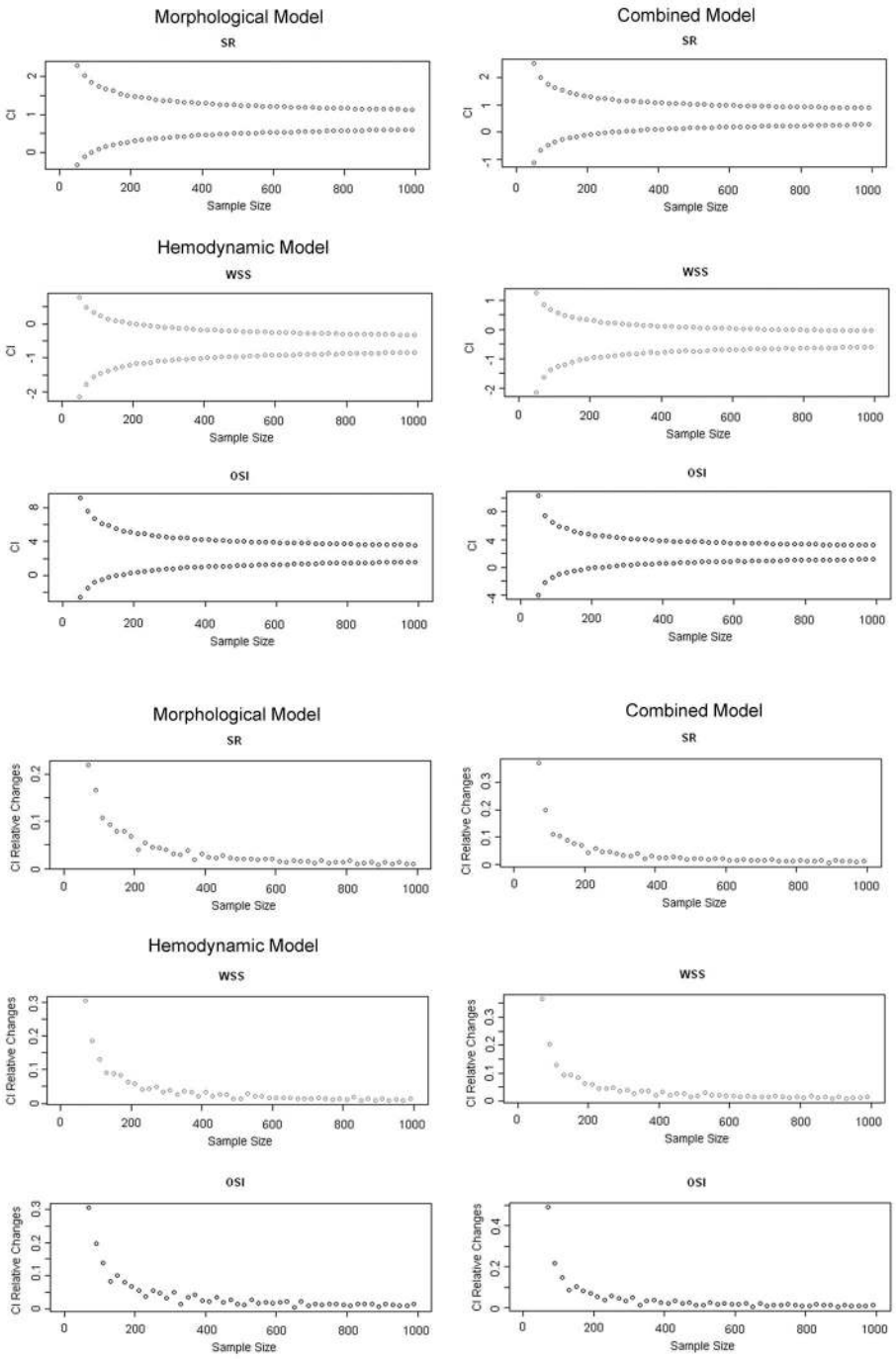

Figure 4.

A: CI width (each step giving lower and upper limits); B: Relative change of CI in the three regression models from the resampling statistical simulations.

Table 1

Demographic information for the testing cohort

Parameter	Ruptured		Unruptured	
Age (yrs, mean±SD)	60.3±15.8		58.9±12.8	
Gender	13F/5M		50F/17M	
Location	Sidewall	Birfucation	Sidewall	Birfucation
ICA	1		31	4
PCOM	5		3	
MCA	1	2	2	6
ACOM		7		13
BA				4
PICA	2		3	
VA			1	
Total	18		67	